Effect of Scale and Mixture Properties on Behaviour of Turbulent Flames in Obstructed Areas

**S. B. Dorofeev, M. S. Kuznetsov,
V. I. Alekseev, A. A. Efimenko,
A. V. Bezmelnitsyn, Yu. G. Yankin,
W. Breitung**

Institut für Neutronenphysik und Reaktortechnik
Projekt Nukleare Sicherheitsforschung
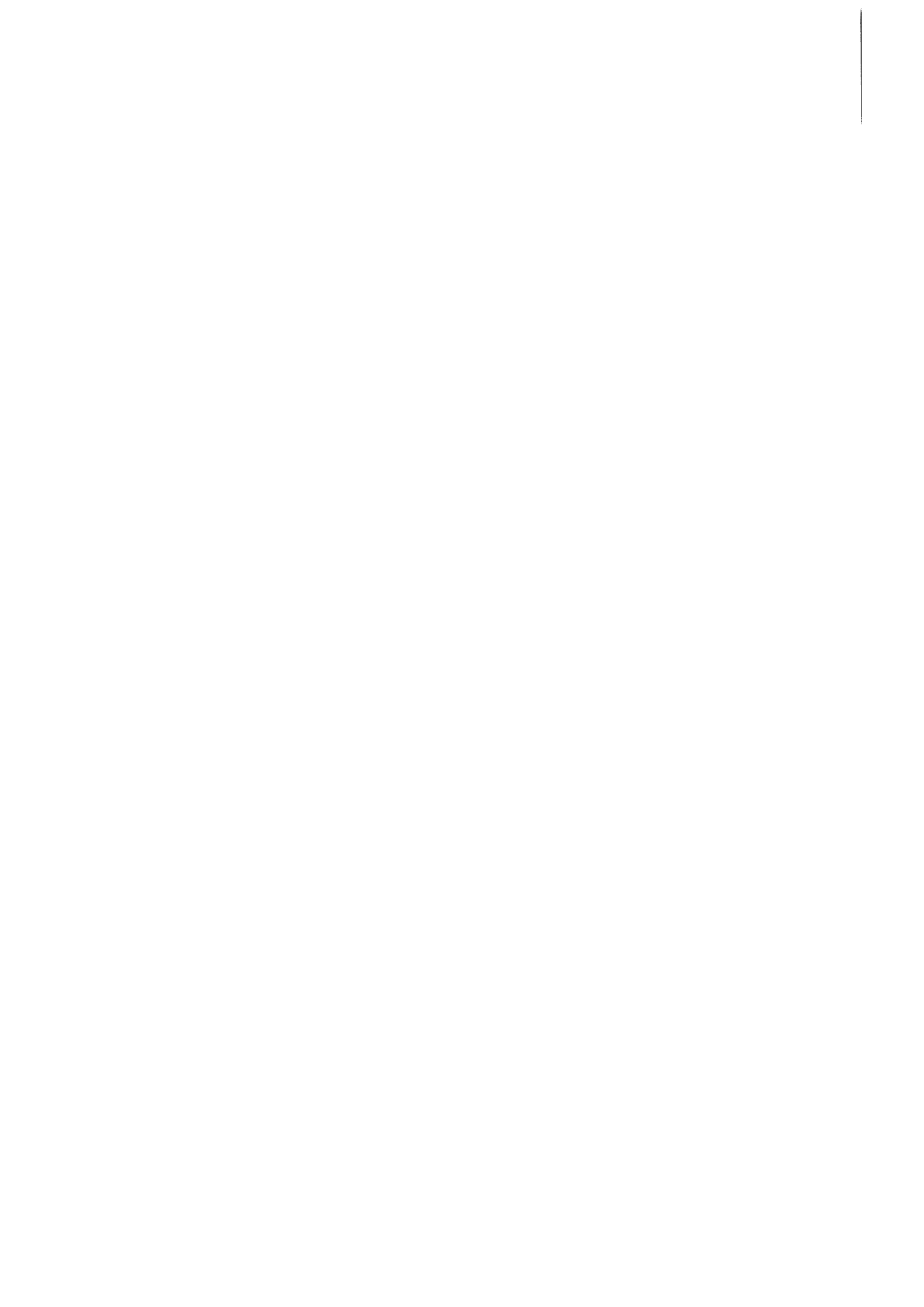
April 1999

Forschungszentrum Karlsruhe

Technik und Umwelt

Effect of Scale and Mixture Properties on Behaviour of Turbulent Flames in Obstructed Areas

S.B. Dorofeev*, M.S. Kuznetsov*, V.I. Alekseev*, A.A. Efimenko*, A.V Bezmelnitsyn*, Yu.G. Yankin* and W. Breitung

Institut für Neutronenphysik und Reaktortechnik

Projekt Nukleare Sicherheitsforschung

* Russian Research Centre "Kurchatov Institute" Moscow, Russia

Abstract

Effect of scale and mixture properties on behaviour of turbulent flames in obstructed areas

Results for the study on the effect of scale and mixture properties on the behaviour of turbulent flames in obstructed areas are presented. A set of dimensionsless parameters was chosen which were defined by the laminar flame speed S_L, the flame thickness δ, the integral length scale L, and thermodynamic mixture properties. The experiments were focused on the study of the effect of these parameters. Two tubes (174 and 520 mm id and similar geometry of obstacles with blockage ratio BR = 0.6) were used in the tests. Different hydrogen mixtures were chosen in order to provide (1) a wide range of the scaling parameters, and (2) combinations with similar values of the parameters at different scales. It was shown that the mixture properties and scale have a mutual effect on the behavior of the turbulent flame. The resulting regime of flame propagation was found to depend mainly on the values of parameter L/δ and expansion ratio σ. It was found that the range of the scaling parameters $L/\delta < 500$, $\sigma < 3.75$ resulted in slow combustion regimes with global quenching. The range $L/\delta > 500$, $\sigma < 3.75$ corresponds to relatively slow and unstable flames. For $\sigma > 3.75$, fast combustion regimes (chocked flames and quasi-detonations) were observed. The expansion ratio σ was found to be the main parameter which defined a border between „weak" (unable to support effective flame acceleration) and „strong" mixtures. The critical value $\sigma \approx 3.75$ found in the present tests should not be considered as universal, but may be a function of Zeldovich and Lewis numbers.

Zusammenfassung

Einfluß von Skala und Mischungseigenschaften auf das Verhalten von turbulenten Flammen in versperrten Geometrien

Der Bericht beschreibt die Ergebnisse einer experimentellen und theoretischen Studie zum Verhalten von turbulenten Flammen in versperrten Geometrien. Für die theoretische Skalierung wurden dimensionslose Parameter abgeleitet, die die laminare Brenngeschwindigkeit S_L, die laminare Flammendicke δ, das integrale Längenmaß der Geometrie L und thermodynamische Größen der Gasmischung enthalten. Die Experimente konzentrierten sich auf die Untersuchung des Einflusses dieser Parameter. Dazu wurden zwei rohrförmige Versuchsanlagen mit 174 bzw. 520 mm Innendurchmesser und einem Versperrungsgrad von 60 % benutzt. Verschiedene Wasserstoff-Inertgasgemische wurden untersucht um 1.) einen großen Bereich für die Skalierungsparameter abzudecken, und 2.) ähnliche Parameterkombinationen auf unterschiedlichen geometrischen Skalen zu erhalten.

Es wurde gezeigt, daß die Mischungseigenschaften und die Abmessung der Umschließung einen wechselseitig abhängigen Einfluß auf die Entwicklung von turbulenten Flammen haben. Das sich einstellende Verbrennungsregime hängt im wesentlichen von den Parametern L/δ und dem Expansionsverhältnis σ der Gasmischung ab. In dem Bereich $L/\delta < 500$ und $\sigma < 3.75$ traten bei Anfangstemperaturen um 300 K nur langsame Verbrennungen mit globalen Löschvorgängen auf. Der Parameterbereich $L/\delta > 500$, $\sigma < 3.75$ entsprach langsamen und instabil brennenden Flammen. Für $\sigma > 3.75$ wurden dagegen nur schnelle Verbrennungsformen wie Überschallflammen und Quasi-Detonationen beobachtet. Das Expansionsverhältnis σ (= Volumen des verbrannten Gases/Volumen des unverbrannten Gases bei konstantem Druck) erwies sich als der Haupteinflußparameter, der die Grenze definiert zwischen „schwachen" Mischungen die nur langsam brennen, und „starken" Mischungen die auf hohe Verbrennungsgeschwindigkeiten beschleunigen. Der hier in Versuchen bei etwa 300 K gefundene kritische Wert von $\sigma \approx 3.75$ stellt keinen universellen Wert dar. Es ist zu erwarten, daß er von der Zeldovich- und der Lewis-Zahl abhängt.

Inhaltsverzeichnis

Nomenclature

Latin

A_{or} - area of the orifice;

A_{fl} - flame surface area;

c_{sr} - sound speed in reactants;

c_{sp} - sound speed in combustion products;

D - diffusion coefficient;

Da - turbulent Damköhler number;

E_a - effective activation energy;

Ka - turbulent Karlovitz number;

L - characteristic geometrical size (e.g., tube diameter);

L_T - integral length scale of turbulence;

Le - Lewis number;

l_K - Kolmogorov length scale of turbulence;

t_K - Kolmogorov time scale of turbulence;

R - gas constant;

Re_T - turbulent Reynolds number;

S_L - laminar flame speed;

S_T - turbulent burning rate;

T - dimensionless time;

T_b - maximum flame temperature;

T_u - initial mixture temperature;

t_T - integral time scale of turbulence;

U - flow speed

V - visible flame speed (laboratory frame);

V_{max} - maximum visible flame speed;

V_{in} -average visible flame speed at initial phase of flame acceleration;

v' - r. m. s. turbulent fluctuations velocity;

X - dimensionless distance;

X_{tr} - dimensionless distance for transition from slow to fast flame phase

Greek

$\beta_d = [diluent]/[O_2]$ - dilution coefficient;

$\beta = E_a(T_b - T_u)/(RT_b^2)$ - Zeldovich number;

γ_r - specific heat ratio in reactants;

γ_p - specific heat ratio in products;

$\delta = S_L\tau = \chi(T_b)/(S_L\sigma)$ - laminar flame thickness;

ν - kinematic viscosity;

σ - ratio of densities of reactants and products (expansion ratio);

χ - temperature conductivity;

τ - characteristic transit time in the laminar flame front.

Introduction

The most dangerous accidental gaseous explosions occur in obstructed areas with significant degree of confinement. Obstructions and confinement provide the most effective means for the flame acceleration and development of hazardous explosion regimes.

Numerous experimental, analytical, and numerical studies have been focused on description of behavior of premixed turbulent flames. Much details can be found in comprehensive reviews on turbulent flames [1-5] and others. Despite the great progress made in development of models for description of turbulent combustion, many practically important problems are still difficult to address with these models. One of these problems is an estimation of severity of an explosion process under given geometrical configuration, scale, and composition of combustible mixture. Such estimates are required for industrial safety applications ranging from offshore platforms to containment of a nuclear power plant. The problem is even not to predict details of turbulent flame propagation under given initial conditions, but rather to give estimations for the maximum possible flame speeds and the corresponding level of overpressures which might be generated during explosion. It is important to know whether the flame is able to accelerate under given conditions resulting in fast turbulent combustion regimes (like "sonic" or "choked" flames [6, 7]) and, possibly, in the transition to detonation, or the flame acceleration is inefficient ending at a benign combustion and even flame quenching.

To provide a foundation for such predictions an adequate description is required of the mutual affect of scale and mixture properties on flame acceleration process. The influence of various factors, including scale, on the flame acceleration was studied extensively (see, e. g., [8-10]). Turbulent burning velocity correlations have been suggested by Abdel-Gayed, Bradley and colleagues [11-13], which include intrinsically the effect of scale and give firm basis for turbulent combustion models. These correlations allow determination of turbulent burning velocities as a

function of dimensionless parameters characterizing turbulence intensity, scale (such as v'/S_L and Re_T) and mixture properties. However, quantitative predictions are not always easy to make, since an additional model is required to determine current level of turbulence in all phases of the process. The problem of scale appeared to be the most challenging task for simplified numerical models of turbulent combustion [14-18]. In the present paper we will try to address this problem experimentally for the case of turbulent flame propagation in obstructed channels.

Scaling parameters

The combustion process itself gives intrinsic length, time, and velocity scales which may be defined by laminar flame thickness δ, characteristic transit time in the laminar flame front τ, and laminar flame speed S_L. Turbulent flow may be characterized by integral length L_T, time t_T, velocity v' scales, and by smallest scales of turbulent spectrum named after Kolmogorov l_K and t_K. The scales L_T, t_T are associated with the most energetic scales of the turbulence spectrum. At high turbulent Reynolds numbers $Re_T = v'L_T/\nu \gg 1$, they appear to be close to large eddy size and turnover time. An interplay between characteristic chemical and turbulent scales is known to result in a variety of turbulent combustion regimes. Following Borghi [19] and Peters [1], characteristic combustion regimes may be displayed diagrammatically using the velocity and length scale ratios as independent variables. The turbulent Damköhler number $Da = t_T/\tau$, the turbulent Karlovitz number $Ka = \tau/t_K$ and turbulent Reynolds number Re_T allow us to identify characteristic regimes of premixed turbulent combustion. Characteristic features of these regimes have been discussed in detail in [1, 5, 19].

Dynamic behavior of a flame propagating from an ignition source is influenced not only by the parameters introduced above. Flame instabilities of different nature may play their roles especially at early stages of combustion, when $v' < S_L$. Flame instabilities combined with flow expansion

4

introduce new scales into the velocity field and cause generation of turbulence, which in its turn effects the combustion regime and burning rate. At a stage characterized by developed turbulence, flame elements appeared to be stretched by turbulence. The response of a flame element to this stretch depends significantly on expansion ratio σ, Zeldovich number $\beta = E_a(T_b - T_u)/(RT_b^2)$, and Lewis number $Le = \chi/D$ [2]. Parameters σ, β, and Le may play their role influencing turbulent burning rate in addition to variables of Borghi diagram. All these factors make extremely difficult an analysis of dynamic behavior of turbulent flames.

The problem of turbulent propagation in an essentially obstructed areas (like a channel with large obstacles), however, allows some simplifications to be made. First of all, the integral scale of turbulence L_T may to be defined by gasdynamic of the flow, that is, by characteristic geometrical size L. The turbulence generation appears to be mainly the result of flow interactions with obstacles through formation of large vortices. A schematic illustration of different stages of flame acceleration in a large channel with obstacles is presented in Fig. 1.

The dynamic behavior of a flame may be qualitatively described as follows. Flame generates the turbulent flow ahead. Interactions of the flow with obstacles result in formation of large vortexes (an example is shown in Fig. 1) which represent essentially large scale turbulent motions. The flame interactions with turbulent motions result in a dominant combustion regime with its characteristic burning rate. While the turbulent burning rate increases with the increase of the turbulence intensity, the interaction of the flame produced flow with the flame itself results in the flame acceleration. In the opposite situation (decrease of burning rate with turbulence intensity), the flame may decelerate. For a given mixture and a given characteristic geometrical size L the dominant combustion regime shifts upward (increasing v'/S_L with nearly-constant L_T/δ) in the Borghi diagram during flame propagation from laminar flamelet area to distributed reaction zones, and, possibly, to quenching area.

The following simple consideration may be useful to identify parameters which influence feedback between flame produced flow and the flame itself. One can assume that the characteristic burning rate S_T at a certain stage of flame propagation is defined approximately by the corresponding combustion regime in Borghi diagram (we are still keeping in mind that σ, β, and Le may play an additional role):

$$S_T/S_L = f(v'/S_L, L_T/\delta). \tag{1}$$

Turbulent Reynolds number appears to be also defined by the position in Borghi diagram and by expansion ratio σ:

$$Re_T = v'L_T/v = (v'/S_L)(L_T/\delta)(\delta/S_L) = (v'/S_L)(L_T/\delta)(\chi(T_b)/v)/\sigma, \tag{2}$$

where $\chi(T_b)$ is temperature conductivity at maximum flame temperature T_b. In writing Eq. 2 we assumed the following obvious expressions for S_L and δ

$$S_L = (\chi(T_b)/\tau/\sigma)^{1/2} \tag{3}$$

$$\delta = (\chi(T_b)\tau/\sigma)^{1/2}, \tag{4}$$

The flame generates a turbulent flow ahead, which will effect the burning rate at the next stage of the flame propagation. The turbulence fluctuations velocity v' representing the most energetic part of the spectrum should be close to characteristic speed in large eddies. Since the formation of large eddies in our case is controlled by flame generated flow around obstacles, the turbulent intensity is defined, generally, by pre-existing level (Eq. 2), and by gasdynamic parameters of the compressible flow, such as sound speeds in the reactants and products (c_{sr}, c_{sp}), and corresponding specific heat ratios (γ_r, γ_p).

The only parameters which appear in our simple consideration are: L_T/δ, S_L, σ, c_{sr}, c_{sp} γ_r, and γ_p (generally, we need to add Zeldovich and Lewis numbers to this set of parameters). One of these

parameters is not independent, because $(c_{sp}/c_{sr})^2 = \sigma\gamma_p/\gamma_r$. Thus, a set of dimensionless parameters may be suggested that are able to effect the flame-flow-flame feedback:

$$L_T/\delta, \ \sigma, \ S_L/c_{sr}, \ S_L/c_{sp}, \ \gamma_r, \ \beta, \text{ and Le.} \tag{5}$$

An important problem, therefore, is to study the effect of these parameters on the behavior of turbulent flames. In the following discussion we will refer to the first 5 parameters as "scaling" parameters and to the last two as "stability" parameters.

The parameters (5) are defined only by mixture properties and scale. They do not include some characteristics of turbulence. The turbulence is supposed to be developed during flame propagation, and this development should be mainly influenced by parameters (5) in the case of large eddy dominated deflagration. This means, for example, that if different mixtures are considered at different scales with similar geometrical configuration and if parameters (5) are kept constant, the flame history is expected to be similar in dimensionless variables $T = t/\tau$ and $X = x/\delta$. Different combinations of parameters (5) are expected to effect characteristic types of turbulent flame behavior. Such a scaling approach is different from others based on preserving dimensionless parameters which include turbulence, like the Karlovitz stretch factor (see, e. g., [20]).

An experimental study on turbulent flame propagation in obstructed areas presented in this paper was focused on the effect of the "scaling" parameters. Two experimental facilities were used to study the effect of scale. Different mixtures were chosen to provide (1) a wide variations of the scaling parameters, and (2) combinations with similar values of the parameters at different scales. The influence of the "stability" parameters was also considered, although it was not the main objective of the study.

Experimental details and mixture properties

Two geometrically similar explosion tubes were used in the tests. DRIVER tube of 174-mm inner diameter and 11.5-m total length was equipped with circular obstacles spaced one diameter apart.

The blockage ratio (BR) was equal to 0.6 in all the experiments. Preliminary evacuated tube was filled with test mixtures prepared by precise partial pressure method in a special mixing tank.

TORPEDO explosion tube of 520-mm inner diameter (33.5 m) long had similar arrangement with circular obstacles spaced one diameter apart (BR=0.6). Test mixtures were prepared inside the tube. The gas components were supplied to each of 22 sections of the pre-evacuated tube. The mixing was due to natural diffusion. The necessary mixing time was defined in the preliminary experiments. Mixture composition was controlled by thermal conductivity sensors. It was found out that test mixtures became homogeneous in approximately 20 hours.

Parameters of pressure waves and flame front (overpressure, signal profile, times of arrival) were recorded using piezoelectric pressure transducers PCB H113A and collimated photodiodes FD-10. A disposition of the pressure and light transducers in both tubes was approximately similar.

The following types of mixtures were used in the tests: H_2-air, $2H_2 + O_2 + \beta_d N_2$, $2H_2 + O_2 + \beta_d Ar$, and $2H_2 + O_2 + \beta_d He$. Hydrogen concentration in air and dilution coefficients β_d were variable. Test conditions are presented in Tables 1 and 2.

Scaling parameters were calculated using tube diameters as the characteristic size L of the tubes. Experimental data on S_L were collected from literature [21-30]. Least squares fits of these data permitted to calculate laminar flame speeds for all mixture compositions used in the tests. Values of δ were calculated from the laminar flame speed and the temperature conductivity using Eq. 4. Values of $\chi(T_b)$ were determined using Ref. [31, 32]. Values of T_b, σ, γ_r, c_{sr}, and c_{sp} were calculated using STANJAN code [33].

Values of main scaling parameters are presented in Tables 1 and 2. It is worth noting that $c_{sp} \approx c_{sr}\sigma^{1/2}$, because $\gamma_r \approx \gamma_p$ for highly diluted and off-stoichiometric mixtures used in the tests. The initial conditions provided a wide range of the scaling parameters. This gives a firm basis for the analysis of the effect these parameters have on the combustion behavior.

Determination of β and Le is not always simple for real mixtures. In the present study, Lewis numbers for lean and reach mixtures were defined by diffusion coefficient of limiting component. For stoichiometric mixtures, Le was determined according to [34]. Lewis numbers are given in Tables 1 and 2.

Effective activation energies E_a were determined from dependence $S_L(T_b)$. The values of E_a/R appeared to be close to 10000K for all mixtures except of rich H_2/air ($E_a/R = 17700K$). Corresponding β-values varied only slightly, from 5 to 7 for all systems, and were in the range $\beta = (10.4 \div 11.4)$ for rich H_2/air mixtures (see Tables 1 and 2).

Experimental results

Typical dependencies of visible flame velocities on distance determined from records of photodiodes are presented in Figs. 2 - 5. Resulting regimes of flame propagation and the final percentage of the fuel burnt are given in Tables 1 and 2.

The slowest flames (referred as "unstable/quench" in Table 1) were observed in 174 mm tube with lean H_2-air and $2H_2+O_2+\beta N_2$ mixtures (Fig. 2). The visible (laboratory frame) speeds of the leading flame tongue were variable along the tube with the maximum value in the range 30-90 m/s. Flames didn't propagate till the end of the tube. The combustion processes were extinguished completely at a certain stage of flame propagation due to interactions with turbulent flow. The combustion processes generated weak pressure waves. The overpressures did not exceed 0.5-0.7 bar. The percentage of the fuel consumed in all the process varied from 10 to 66% in these experiments.

The unstable and relatively slow regime with local quenching and reignition (referred as "unstable/slow" in Tables 1 and 2) was observed in the lean hydrogen-air mixtures in both 174-mm and 520-mm tubes (Figs. 2 and 4). The visible speeds of the leading flame tongue were variable along the tube with the maximum value in the range 100 - 200 m/s. As different from the previous

9

regime, flames reached the end of the tube. An example of a detailed (x-t)-diagram of flame propagation in this regime is shown in Fig. 5. At certain conditions a local quenching is observed. It is followed by a reignition downstream. Flame propagates both upstream and downstream from reignition points. Pressure waves formed in these processes were stronger compared to the first regime with local overpressures 2-5 bar due to galloping character of flame propagation.

The regime of fast flame acceleration resulted in the choked flames (referred as "choked flames" in Tables 1 and 2) was observed in all types of mixtures at high enough hydrogen concentrations. The final steady-state flame speed ranged from 70 to 80% of the sound speed in combustion products. Flame propagation was accompanied by strong pressure waves (overpressures about 6-8 bar).

Processes of fast flame acceleration resulted in choked flames and transition to quasi-detonation was observed in He-diluted and Ar-diluted mixtures (see Tables 1 and 2). A discussion of critical conditions for DDT is beyond the scope of this paper.

A comparison of results in 174mm and 520mm tubes shows that the range of hydrogen concentrations, at which slow flames can be expected (between flammability limit and a limit of fast flames), becomes smaller with the scale increase. Such a "slow flames gap" was not observed at all for rich hydrogen/air mixtures and for mixtures diluted with Ar and He. In these mixtures, either the flame accelerated very rapidly, or ignition was not achieved.

Discussion

To analyze the effect of the scaling parameters, the experimental data on turbulent flame propagation were scaled with δ and $\tau = S_L/\delta$. A characteristic (X-T)-diagram of the flame propagation in dimensionless coordinates $X = x/\delta$ and $T = tS_L/\delta$ is presented in Fig. 6. The data from three tests with close values of parameters L_T/δ, σ, and S_L/c_{sp} are shown. Stability parameters were also not much different for these mixtures (Tables 1 and 2). The flame trajectories in the dimensionless coordinates are very similar. Some other pairs of mixtures show similarity of the

flame propagation in 174 mm tube. This is an important observation; however, not much conclusions can be drawn out just from a few examples of the similarity. An analysis based on the overall picture of the flame propagation, is difficult, because too many parameters are involved. It seems more productive to look at separate phases of the process, and to focus on those parameters that are important for each of these phases. The characteristic phases of the processes may be distinguished as shown in Fig. 6.

The first phase is characterized by relatively slow flame acceleration. The flame speed is much lower than the sound speeds c_{sr} and c_{sp}. The main scaling parameters for this phase should be L/δ and σ. The second phase is the fast acceleration phase. It was relatively very short in all the tests made. During this phase the flame speed changes rapidly from essentially subsonic values to nearly-sonic, or supersonic ones. Depending on the initial conditions, flame quenching, relatively slow unstable flames, choked flames, or quasi-detonations are characteristic regimes in the final phase. Characteristic parameters of the flame propagation process are shown in Fig. 6. These are the initial average speed before transition to the final phase V_{in}, the transition distance X_{tr}, and the maximum propagation speed V_{max}.

Figure 7 shows that the speed V_{in} is defined approximately by the values of L/δ and σ. For each group of the values of σ, the V_{in}-value increases with L/δ. An extrapolation to $L/\delta = 0$ gives V_{in}-values close to the visible laminar flame speed $S_L\sigma$. This indeed should be expected at small scales, where Reynolds numbers are small and the turbulence is not developed. The different values of γ_r, c_{sr}, and c_{sp} do not effect significantly the flame propagation in this phase.

Determination of the dimensionless transition distance X_{tr} showed that all the experimental points with different σ, γ_r, c_{sr}, and c_{sp} are grouped very closely around one line $X_{tr} = 2L/\delta$. This means that in all the tests the resulting combustion regime was formed just after second obstacle. The time to transition was proportional to the characteristic chemical time $\tau = \delta/S_L$.

The dependence of the maximum flame velocities V_{max} on L/δ is presented in Fig. 8. The values of V_{max} are normalized with c_{sp} in order to better distinguish a level of flame speeds. As expected, the maximum propagation velocities of choked flames and quasi-detonations are defined by c_{sp}. Maximum velocities of slow and unstable flames clearly increase with L/δ. Figure 8 shows that $L/\delta \approx 500$ is an approximate borderline between cases of global quenching and unstable flames.

The dependence of the maximum flame velocities V_{max} on σ is presented in Fig. 9. Relatively slow flames are observed only for $\sigma < 3.75$. Thus, Figs. 8 and 9 show that areas of parameters can be distinguished that define initial conditions causing different behavior of turbulent flames. This is illustrated by Fig. 10. The range of the scaling parameters $L/\delta < 500$, $\sigma < 3.75$ results in regimes with global quenching. The range $L/\delta > 500$, $\sigma < 3.75$ corresponds to relatively slow and unstable flames. For $\sigma > 3.75$, fast flames may be expected.

What turbulent combustion regimes were observed in the tests in terms of the Borghi diagram? To find combustion regimes on the diagram one needs to have values of v'. A rough estimate of v' can be made using average visible flame speed V given by V_{in} or V_{max} (depending on the phase of the process). Indeed, the flow speed U in an obstacle orifice can be estimated as $U = (\sigma - 1)/\sigma \cdot V \cdot A_{fl}/A_{or}$. Flame spreads along the tube as a result of burning plus expansion of combustion products, while across the tube it is not affected by expansion. This gives an estimate for $A_{fl}/A_{or} \approx \sigma/BR \approx 10$ (BR = 0.6). Assuming v' $\approx 0.1U$, one can estimate v' by the order of magnitude as v' $\approx$ V.

Figure 11 shows combustion regimes observed experimentally in variables of the Borghi diagram. Although the values of v' are estimated by the order of magnitude only, some important features can be revealed in Fig. 11. The initial stage of the flame acceleration corresponds to the flamelet regime (Ka > 1). During the second phase, the turbulent combustion regime shifts rapidly to the

12

region where Da is of the order of unity, and quenching should be expected. The global or local quenching was indeed observed in the tests corresponding to the upper group of points in Fig. 11. Local flame quenching should be also typical for choked flames. The quenching itself, consequently, does not necessarily mean that fast flames cannot be developed. High propagation velocity can be due to gasdynamic processes as it is the case for choked flames. The border between fast and slow flames should be defined by additional parameters which are not used explicitly in the Borghi diagram. The results of the present discussion suggest that expansion ratio σ is the most important parameter which makes possible to divide mixtures into "weak" and "strong". Flame acceleration can be very efficient in "strong" (large σ) mixtures, while it is suppressed in "weak" (small σ) mixtures, even under favorable conditions.

The importance of σ as a parameter for flame acceleration is not just due to the fact that σ is approximately equal to the ratio of the chemical energy release to the initial thermal energy. Increase of σ results in strong non-linear increase of the possible flame speeds, because convection is proportional to σ, effective flame surface area increases with σ, and, generally, S_T increases with σ, as well, through increase of flow speed and turbulence level.

Is σ the only parameter defining ability of a mixture to support effective flame acceleration? The results presented here do not show explicitly some significant effect of other parameters, including stability parameters β and Le. However, the slow/fast flames border was actually identified for lean H_2/air and for stoichiometric $H_2/O_2/N_2$ mixtures (in other mixtures the only fast flames were observed). For these mixtures, Le number was either close to 0.3 or 1, and β was almost constant and close to 6.5. The combination $\beta(Le - 1)$, which defines the border for thermal-diffusive flame instability was around two distinct values $\beta(Le - 1) \approx -4$ and $\beta(Le - 1) \approx -0.5$, which are below and above the stability threshold $\beta(Le - 1) \approx -2$. Such a limited range of parameters is, probably,

insufficient to determine the possible effect of Le number and, especially, β on flame acceleration efficiency. Thus, the critical value of $\sigma \approx 3.75$ should not be considered as a universal constant. Changes of the critical σ-value may be principally expected in mixtures with different values of β and Le.

Experimental data of Ciccarelly et al. [35] for hydrogen mixtures at elevated initial temperature give a possibility to estimate the effect of β. For $T_u = 300K$, fast flames were observed in [34] only in mixtures with $\sigma > 3.7$. This is in accord with the critical value of $\sigma \approx 3.75$ found in our study, although the geometrical configuration in [34] was different. For elevated initial temperatures, data [34] give the following critical values: $\sigma \approx 2.8$ for $T_u = 400K$ ($\beta \approx 5.5$), $\sigma \approx 2.2$ for $T_u = 500K$ ($\beta \approx 4.5$), and $\sigma \approx 2.1$ for $T_u = 650K$ ($\beta \approx 3.6$). These estimates show that more detailed analysis is required to evaluate effect of Le and β on efficiency of flame acceleration.

Conclusions

Mixture properties and scale were shown to have a mutual effect on the behavior of the turbulent flames. In connection with safety problems, it was found that the range of hydrogen concentrations at which slow flames can be expected (between the flammability limit and a limit of fast flames) becomes narrower with the scale increase. Slow flames were not observed at all in rich hydrogen-air mixtures and in mixtures diluted with Ar and He.

The analysis based on the scaling parameters was found to be able to give useful results. It was observed that the trajectories of the flame propagation were similar in dimensionless coordinates x/δ, t/τ, with approximately similar values of L/δ, σ, and S_L/c_{sp}. In the initial phase of the flame acceleration (which was in the flamelet regime), the parameters L/δ and σ were shown to be the most important defining average speed of the flame propagation and characteristic distance for flame acceleration.

14

A relative strength of combustion regimes resulting from flame acceleration in a sufficiently long obstructed tubes was found out to depend on the combination of L/δ and σ. The range of the scaling parameters L/δ < 500, σ < 3.75 resulted in slow combustion regimes with global quenching. The range L/δ > 500, σ < 3.75 corresponded to relatively slow and unstable flames. For σ > 3.75, fast combustion regimes (choked flames and quasi-detonations) were observed.

The sum of the results suggests that mixture properties give parameters which allow to classify the mixtures as "strong" and "weak" depending on their ability to support effective flame acceleration under favorable conditions. The expansion ratio σ was found to be the main parameter which defined a border between weak and strong mixtures in the present series of tests. The critical value σ > 3.75, however, should not be considered as a universal threshold for effective flame acceleration. It is expected that critical σ value may be a function of β and Le. Variations of these parameters were insufficient in the present tests to estimate their role systematically.

The critical threshold for effective flame acceleration may be also a function of the geometrical configuration. The configuration used in the present tests was very favorable for an efficient flame acceleration. This suggest that estimations of possible strength of explosion processes based on the results presented here should be conservative. However, additional experiments and analysis are required to evaluate the range of applicability of the criteria suggested in this study.

References

1. Peters N., *21ˢᵗ International Symposium on combustion*, The Combustion Institute, Pittsburgh, 1986, pp. 1231-1250.

2. Clavin, P., *Prog. Energy Combust. Sci.* 11: 1-59 (1985)

3. Bradley, D., *25ᵗʰ International Symposium on combustion*, The Combustion Institute, Pittsburgh, 1992, pp. 247-262.

4. Libby, P. A. and Williams, F. A., Eds., Turbulent reacting flows, Academic Press, London, 1994.

5. Bray, K. N. C., *26th International Symposium on combustion*, The Combustion Institute, Pittsburgh, 1996, pp. 1-26.

6. Chan, C. K., Moen, I. O., and Lee, J. H., *Combust. Flame* 49:27 (1983).

7. Lee, J. H., Knystautas, R., and Chan, C. K., *20th International Symposium on combustion*, The Combustion Institute, Pittsburgh, 1984, pp. 1663-1672.

8. Moen, I. O. Lee, J. H. S., Hjertager, B. H., Fuhre, K., and Eckhov, R. K., *Combust. Flame*, 47: 31 (1982)

9. Moen, I. O., Donato, m., Knystautas, R., Lee, J. H. S., and Wagner, H. Gr. In: *Prog. Astronautics and Aeronautics* 75: 31 (1981)

10. Hjertager, B. H., Bjørkhaug, M., and Fuhre, K., *J. Loss Prev. Proces. Ind.,* 1: 197-205 (1988).

11. Abdel-Gayed, R. G., Al-Khishali, K. J., and Bradley, D., *Proc. R. Soc. Lond.* A 391: 393-414 (1984)

12. Abdel-Gayed, R. G., and Bradley, D., *Combust. Flame* 62: 61-68 (1985)

13. Bradley, D., Lau, A. K. C., and Lawes, M., *Phyl. Trans. Proc. R. Soc. Lond.* A 338: 359-387 (1992)

14. Hjertager, B. H., *Combust. Sci. Technol.,* 41: 159-170 (1982)

15. Hjertager, B. H., *J. Hazardous Materials,* 34:173-197 (1993)

16. Hjertager, B. H., Sæter, O., and Solberg, T., Pre-prints of the 2nd International Specialist Meeting on Fuel-Air Explosions, Bergen, Norway, 1996, p. 5.1 - 5.14.

17. Kotchourko, A. S., Dorofeev, S. B., Breitung, and Sidorov, V. P., *Proceedings of 16th ICDERS*, Poland, Cracow, 1977, p.465.

18. Kotchourko, A. S., Breitung, W., Veser, A., and Dorofeev, S. B., *Proceedings of 21st International Symposium on Shock waves*, Great Keppel, Australia, 1997, p. 231.

19. Borghi R., in Recent Advances In Aerospace Science (Bruno, C. and Casci, C., Eds.) Plenum Press, N. Y., 1985, p117.

20. Catlin, C. A. and Jonson, D., M., *Combust. Flame* 88: 15-27 (1992)

21. Koroll G. W., S. R. Mulpuru. *21st International Symposium on combustion,* The Combustion Institute, 1986, pp. 1811-1919

22. Koroll G. W., R. K. Kumar, E. M. Bowles. *Combust. Flame* 94: 330-340 (1993)

23. Gunther R., and G. Janish, *Combust. Flame* 19: 49-53 (1972)

24. Liu D. D. S., and R. McFarlane, *Combustion and Flame* 49: 59-71 (1983)

25. Andrews G. E., and D. Bradley, *Combust. Flame* 20: 77-89 (1973)

26. Berman M. Sandia Laboratories Report, SAND84-0689, 1984.

27. Karpov V. P., E. S. Severin, *Fizika Goreniya i Vzryva,* Vol. 16, No 1 (1980) - in russian

28. Babkin V. C., A. V. V'yun, *Fizika Goreniya i Vzryva,* 7:3(1971) - in russian

29. Coward H., and W. Payman, *Chem. Rev.,* 21:359 (1937)

30. Coward H., and G. Jones, *J. Am. Chem. Soc.,* 49:386 (1927)

31. Reid R. C., J. M. Prausnitz, T. K. Sherwood. The properties of gases and liquids, 3rd edition, McGraw-Hill Bok Company, NY, London, Tokyo, 1976.

32. Vargaftic N. B. Thermo-physical properties of gases and liquids. (Handbook), Moscow, "Nauka" Publishers, 1972, 720 p.

33. Reynolds, W.C., The Element Potential Method for Chemical Equilibrium Analysis: Implementation in the Interactive Program STANJAN Version 3, Dept. of Mechanical Engineering, Stanford University, Palo Alto, California, January 1986.

34. Joulin G. and T. Mitani. *Combust. Flame* 40: 235-246 (1981)

35. Ciccarelly G., J. Boccio. T. Ginsberg, C. Finfrock, L. Gerlach, H. Tagava, and A. Malliakos. The Effect of Initial Temperature on Flame Acceleration and Deflagration-to-Detonation Transition Phenomenon. NUREG/CR-6509, BNL-NUREG-52515, 1998.

Table 1.

Properties of mixtures and results of 174-mm tube experiments

Mixture	β_d	H_2, % vol.	σ	L/δ	10^3 S_L/c_{sr}	β	Le	Fuel burnt[a,b] %	Resulting combustion regime [a]
H_2/air		9	3.31	450	0.48	6.9	0.34	35-57	Unstable/quench
H_2/air		9.5	3.43	530	0.58	6.7	0.35	15-47	Unstable/quench, Unstable/slow
H_2/air		10	3.54	600	0.68	6.6	0.35	14-66	Unstable/quench, Unstable/slow
H_2/air		10.5	3.66	680	0.80	6.4	0.36	65-82	Unstable/slow
H_2/air		11	3.77	750	0.92	6.3	0.36	70-81	Choked flame
H_2/air		11.5	3.88	830	1.1	6.2	0.36	60-85	Choked flame
H_2/air		12	3.99	910	1.2	6.0	0.37	75-83	Choked flame
H_2/air		13	4.21	1100	1.5	5.8	0.38	74-76	Choked flame
H_2/air		15	4.63	1300	2.1	5.3	0.39	71.2	Choked flame
H_2/air		70	4.24	600	1.6	10	3.8	69-89	Choked flame
H_2/air		70.5	4.19	560	1.5	11	3.8	87	Choked flame
H_2/air		70.75	4.17	540	1.4	11	3.9	82-85	Choked flame
H_2/air		71	4.14	520	1.3	11	3.9	84-85	Choked flame
H_2/air		72	4.05	450	1.1	11	4.0	86-92	Choked flame
H_2/air		75	3.76	250	0.60	11	4.2	87	Choked flame
H_2/O_2/N_2	17	10	3.56	250	0.24	6.9	0.92	7	Unstable/quench
H_2/O_2/N_2	16.05	10.5	3.68	280	0.28	6.8	0.94	10-57	Unstable/quench
H_2/O_2/N_2	15.18	11	3.79	310	0.32	6.6	0.95	62	Unstable/quench
H_2/O_2/N_2	14.39	11.5	3.90	340	0.37	6.5	0.96	84-85	Choked flame
H_2/O_2/N_2	12.8	12.7	4.17	430	0.50	6.2	0.98	79	Choked flame
H_2/O_2/N_2	10.33	15	4.66	620	0.81	5.7	1.0	83	Choked flame
H_2/O_2/He	16.05	10.5	4.73	210	0.60	6.1	1.8	81.2	Choked flame
H_2/O_2/He	15.18	11	4.89	240	0.69	6.0	1.8	80-82	Choked flame
H_2/O_2/He	12.39	13	5.47	370	1.2	5.4	1.7	81	Choked flame
H_2/O_2/He	10.33	15	5.99	550	1.9	5.0	1.7	84	Quasi-detonation
H_2/O_2/Ar	20.53	8.5	4.09	380	0.43	7.1	0.98	72	Choked flame
H_2/O_2/Ar	19.86	8.75	4.18	400	0.46	7.0	0.99	75-77	Choked flame
H_2/O_2/Ar	19.22	9	4.26	430	0.50	6.9	0.99	79	Choked flame
H_2/O_2/Ar	17	10	4.58	550	0.69	6.5	1.0	85	Choked flame
H_2/O_2/Ar	15.18	11	4.88	680	0.91	6.2	1.1	82	Choked flame
H_2/O_2/Ar	13.67	12	5.18	820	1.2	5.9	1.1	79-83	Quasi-detonation
H_2/O_2/Ar	12.39	13	5.47	980	1.5	5.6	1.1	80-82	Quasi-detonation

[a]) Most of tests were repeated at least twice with similar mixture composition. Portion of fuel burnt and, in some cases, combustion regime varied from test to test.

[b]) Oxygen consumed for rich mixtures

Table 2.

Properties of mixtures and results of 520-mm tube experiments.

Mixture	β_d	H_2, % vol.	σ	L/δ	$10^3 S_L/c_{sr}$	β	Le	Fuel burnt, %	Resulting combustion regime
H_2/air		9	3.31	1350	0.48	6.9	0.34	68	Unstable/slow
H_2/air		9	3.31	1350	0.48	6.9	0.34	39	Unstable/slow
H_2/air		9	3.31	1350	0.48	6.9	0.34	60	Unstable/slow
H_2/air		9	3.31	1350	0.48	6.9	0.34	35	Unstable/slow
H_2/air		9.5	3.43	1570	0.58	6.7	0.35	70	Unstable/slow
H_2/air		10	3.54	1790	0.68	6.6	0.35	88	Unstable/slow
H_2/air		10	3.54	1790	0.68	6.6	0.35	76	Unstable/slow
H_2/air		10.9	3.77	2250	0.92	6.3	0.36	93	Choked flame
H_2/O_2/He	15.2	11	4.89	717	0.69	6.0	1.8	88	Choked flame
H_2/O_2/He	14.4	11.5	5.04	807	0.80	5.8	1.7	88	Choked flame
H_2/O_2/He	14.4	11.5	5.04	807	0.79	5.8	1.7	84	Quasi-detonation

List of Figures

Figure 1. Examples of shadow photographs of different regimes of turbulent flame propagation in obstructed channels. Initial stage of flame acceleration (upper), large eddy dominated flame (center), and choked flame (lower).
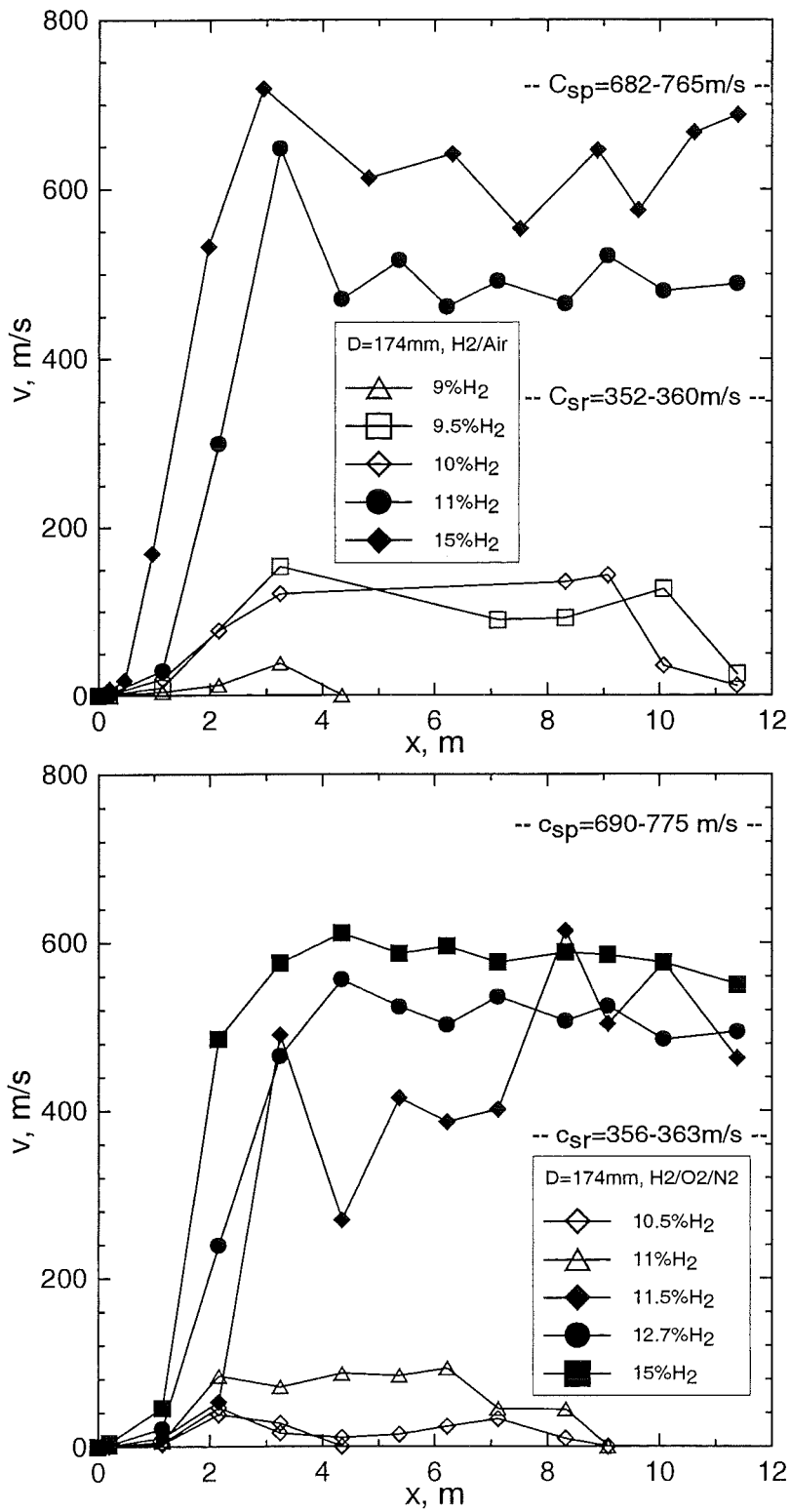
Figure 2. Flame propagation speed versus distance along the tube. For slow combustion regimes (empty points) speed of flame head is given. Tests with hydrogen-air (upper plot) and $H_2/O_2/N_2$ (lower) mixtures in 174 mm tube.
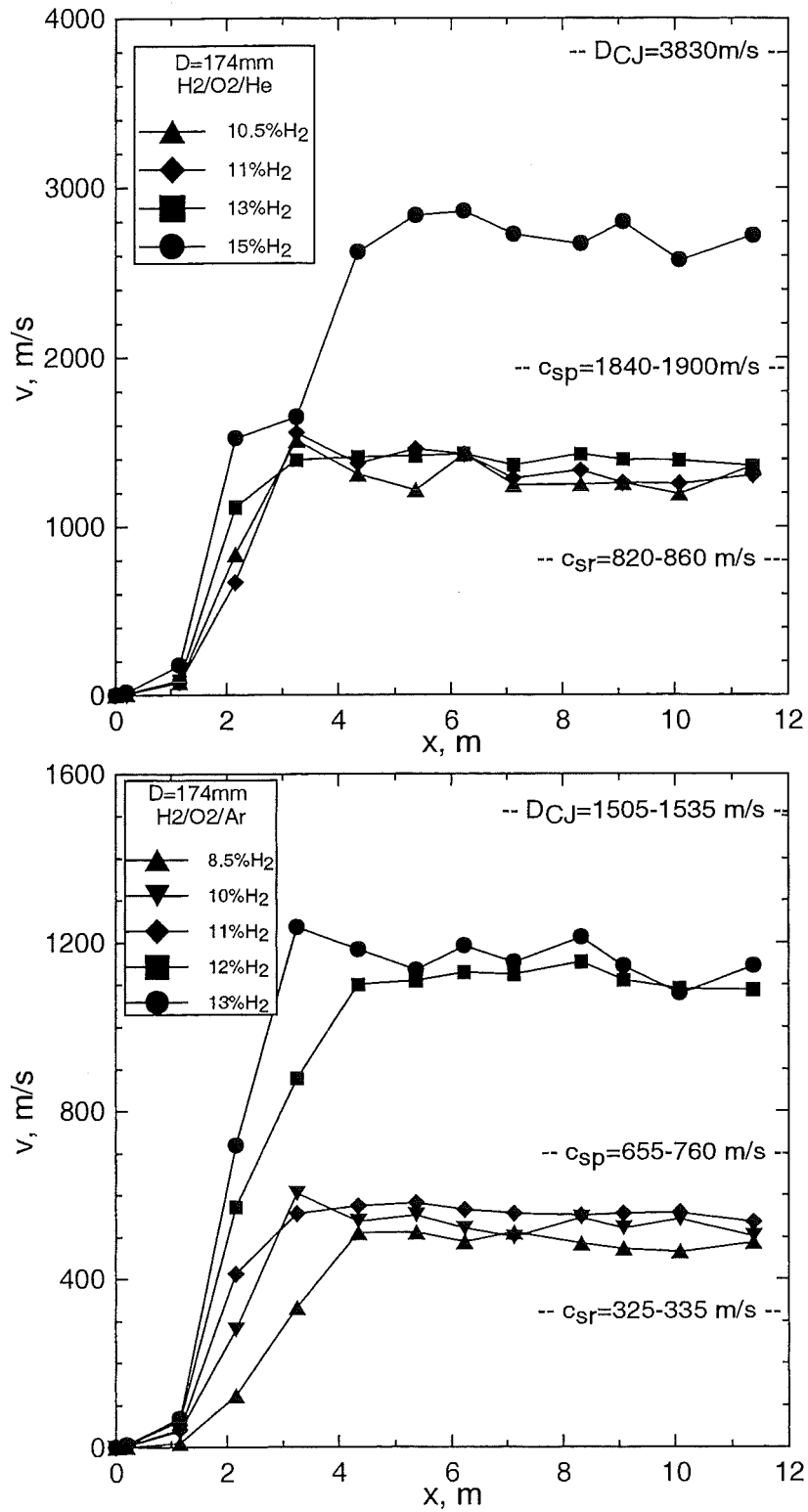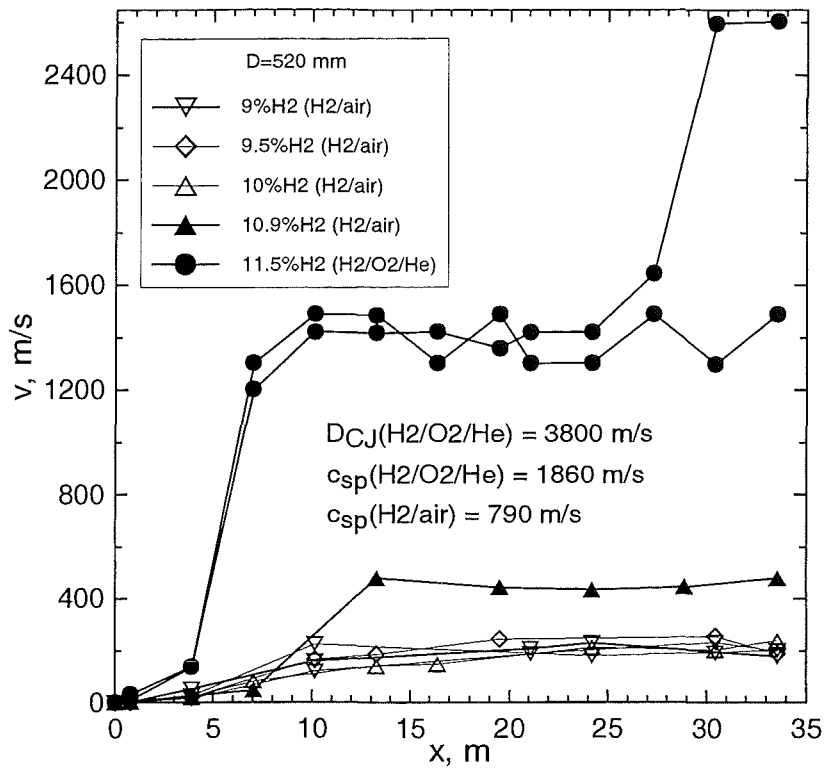
Figure 3. Flame propagation speed versus distance along the tube. Tests with $H_2/O_2/He$ (upper plot) and $H_2/O_2/Ar$ (lower) in 174 mm tube.

Figure 4. Flame propagation speed versus distance along the tube. For relatively slow combustion regimes (empty points) speed of flame head is given. Tests with $H_2/O_2/He$ and H_2/air mixtures in 520 mm tube.
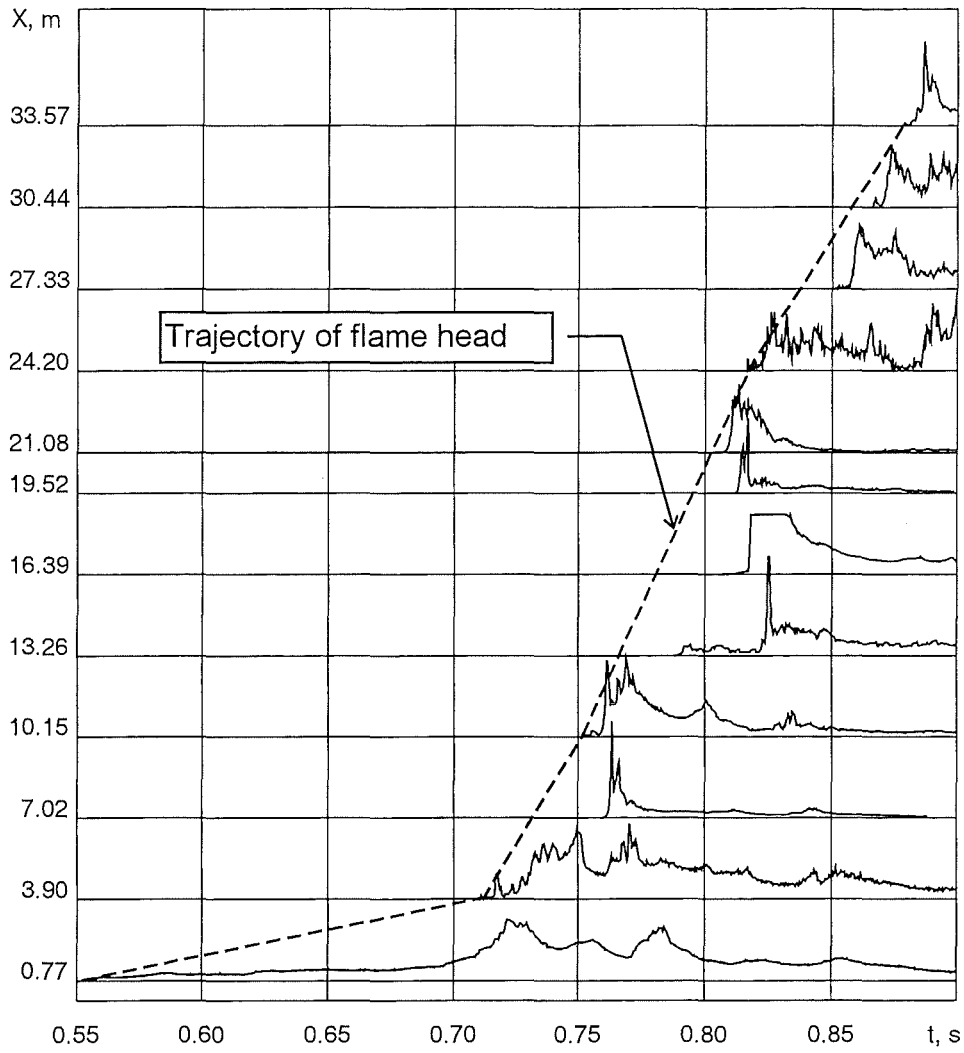
Figure 5. X-t diagram of flame propagation in 9% H_2/air mixture in 520-mm tube. Records of photodiodes.
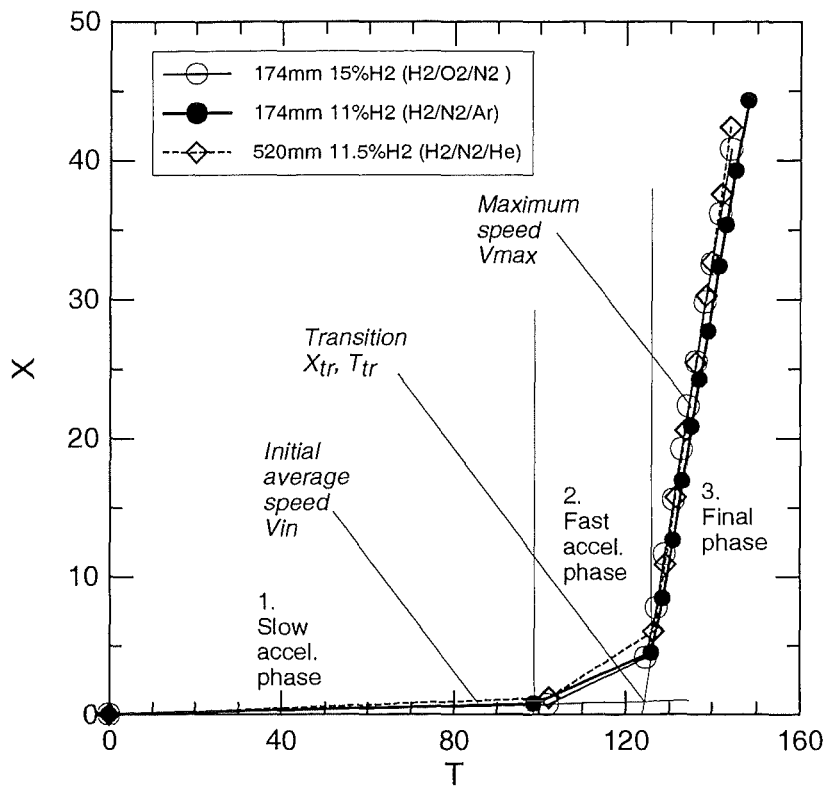
Figure 6. Characteristic dimensionless X-T-diagram of flame front propagation,
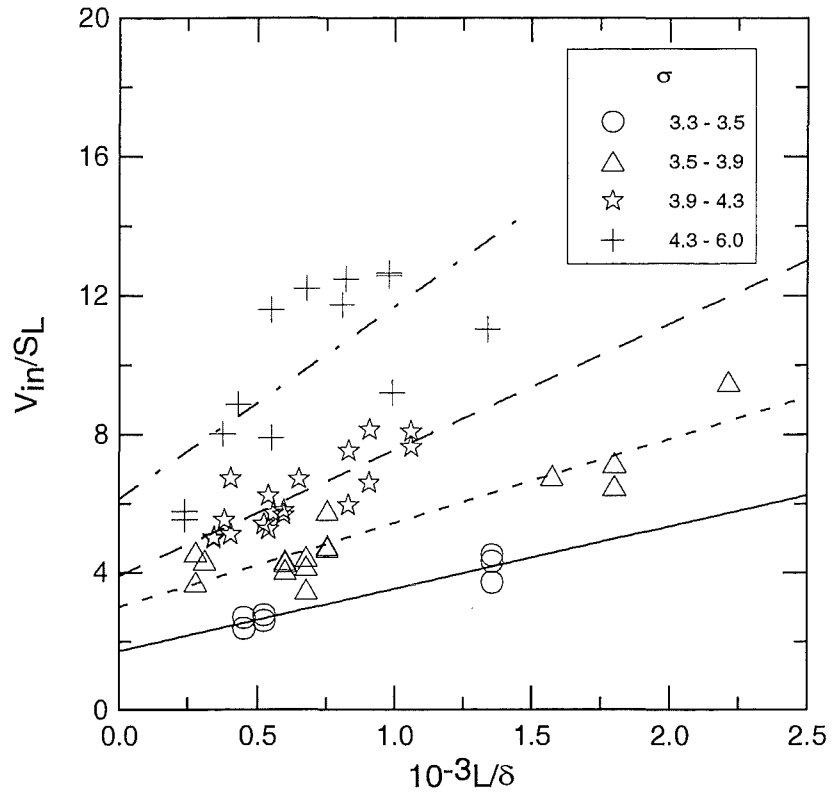
Figure 7. Dimensionless average flame speed in the initial phase versus scaling parameter L/δ for different values of σ. Points -experimental data, lines - linear approximations.
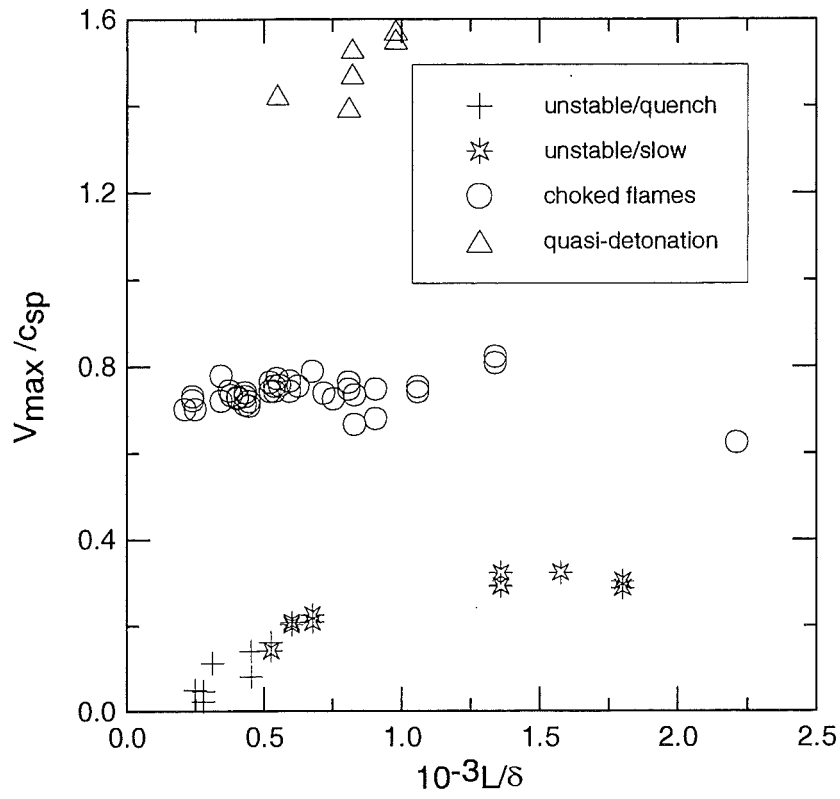
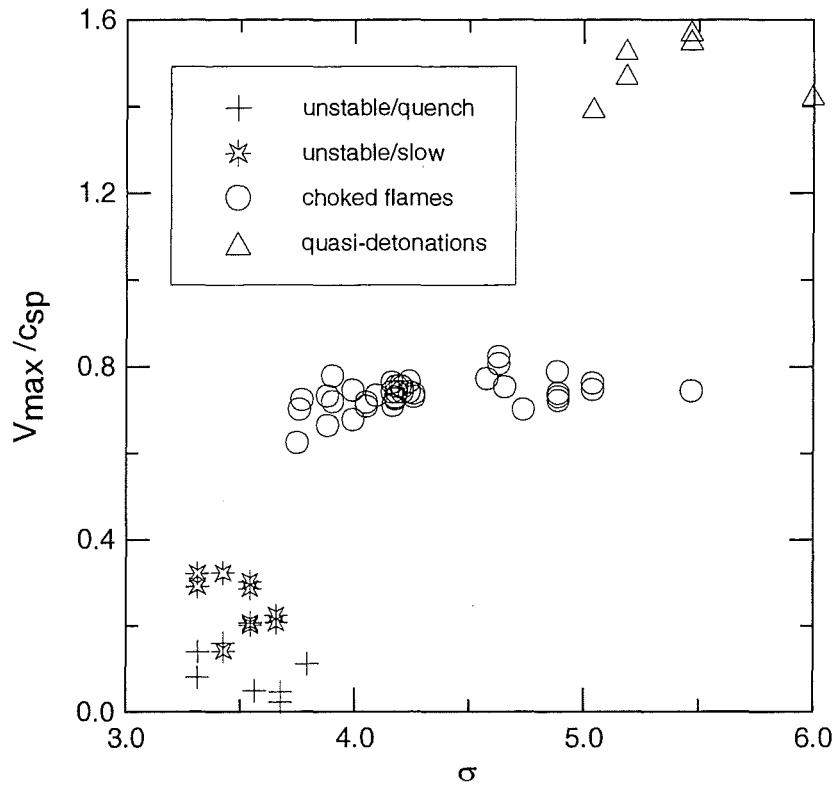Figure 8. Maximum flame speeds in the final phase of the flame propagation versus scaling parameter L/δ.

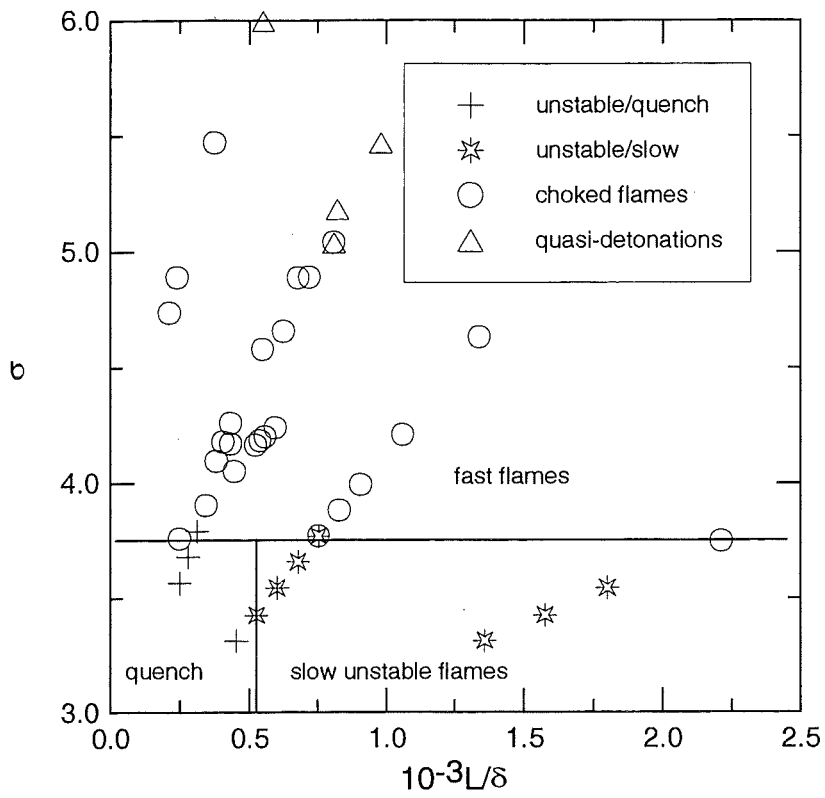Figure 9. Maximum flame speeds in the final phase of the flame propagation versus σ.

Figure 10. Resulting combustion regime as a function of scaling parameters L/δ and σ.
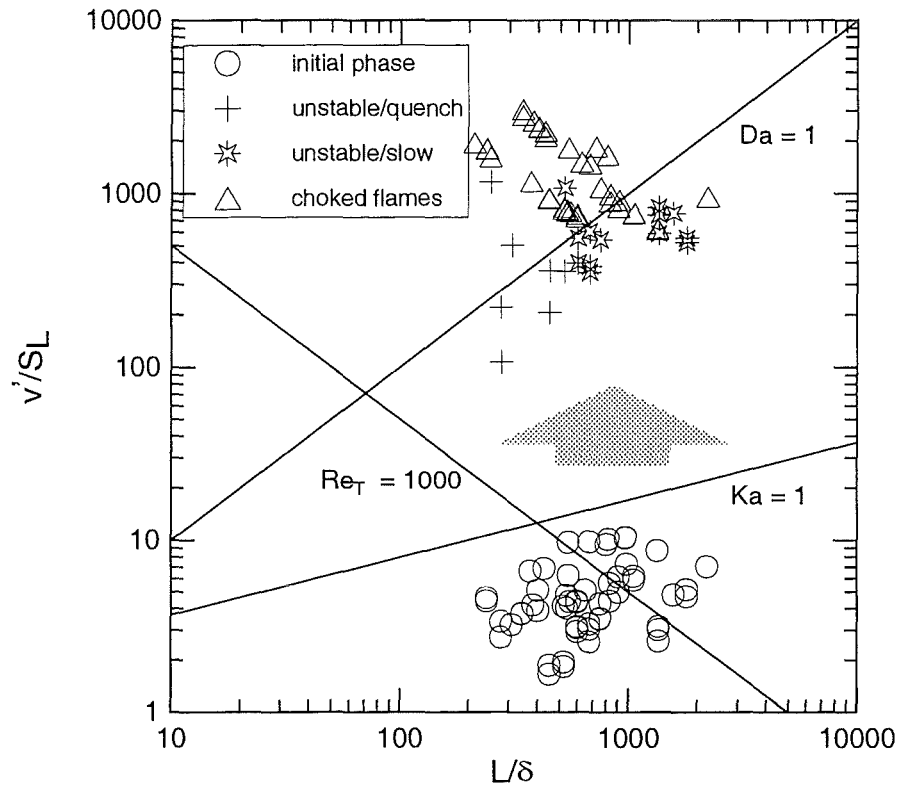
Figure 11. Turbulent combustion regimes observed experimentally in Borghi diagram.